Preliminary version

SIMULATION OF NATURAL CONVECTION IN A SIDE-HEATED CAVITY WITH A NEAR-CRITICAL FLUID

Vadim I. Polezhaev, Elena B. Soboleva

Institute for Problems in Mechanics, Russian Academy of Sciences
Prospect Vernadskogo, 101, b.1, 117526 Moscow, Russia
Tel: 007-095-434-3283, Fax: 007-095-938-2048, E-mail: soboleva@ipmnet.ru

Numerical simulation of the thermal gravity-driven convection near the thermodynamic critical point in a square cavity with side heating is performed. Governing equations of the non-perfect gas (Navier-Stokes equations with equation of energy) in approximation to low-speed flows with van der Waals equation of state are used. The "real" dimensionless parameters based on the near critical properties are introduced. Near critical fluid and perfect gas with "real" parameters are compared under unsteady and steady conditions. It was obtained that unsteady dynamics of two media is different but in steady flows there is some analogy.

Thermal gravity-driven and vibrational convection of the near critical fluid in microgravity is simulated. It was shown that vibrations with sufficiently small values of frequency and amplitude may induce the average convective motion. Numerical results are compared with results of experiments on MIR station. These results allow to qualitatively interpret experimental optical pictures, obtained in near-critical fluid after heat pulse input.

Near-critical properties

Near-critical fluid is characterized by the temperature and pressure which are close to these values in the thermodynamical critical point. Under these conditions fluid displays specific static and dynamical properties. Static critical properties (asymptotic discrepancy of the constant-pressure heat capacity, coefficients of isothermal compressibility and heat expansion) relate with equation of state in which first and second derivatives $\partial p/\partial \rho$ and $\partial^2 p/\partial \rho^2$ in the critical point must be zero (p - pressure, ρ - density). Dynamical critical properties include the anomalistic behavior of the transport coefficients, for example, large increasing of the thermal conductivity [1]. These peculiar properties lead to certain different features in heat and mass transfer in compared with perfect gas. It is known that in enclosures temperature may propagates very fast as a result of the piston-effect [2] obtained numerically in 1D- [3], [4] and 2D-simulation [5].

Thermal gravity-driven convection is characterised by Rayleigh number Ra_r and Prandtl number Pr_r. If external mass force is varied quickly or cavity with fluid oscillates the vibrational convection is induced; it is described by vibrational Rayleigh number Rv_r. Undimensional criteria above include the real parameters of the near-critical fluid and signed by subscript "r". For the fluid with density ρ' and viscosity η' in the cavity with size l' and temperature difference Θ' they are defined as

$$Ra_r = \theta'\beta' g' l'^3 \rho'^2 c'_p/(\lambda'\eta'), \quad \mathrm{Pr}_r = c'_p \eta'/\lambda', \quad Rv_r = \frac{1}{2}\frac{(A'\omega'\beta'\Theta' l')^2 \rho' c_p'}{\lambda'} \tag{1}$$

Fluid is affected by static mass force g' and oscillations with frequency ω' and amplitude A'; primes represent dimensional values. Coefficient of heat expansion β' and constant-pressure heat capacity c'_p increase in near-critical region and defined by equation of state

$$\beta' = -1/\rho' (\partial \rho'/\partial T')_{p'}, \quad c'_p = c'_v + T'/\rho'^2 (\partial p'/\partial T')^2 \rho' (\partial \rho'/\partial p')_{T'} \tag{2}$$

In this investigation equation of state in form Van der Waals equation is taken into account but it may be different [6]. For this form the «real» parameters become the follows (we consider critical isochor)

$$Ra_r = \frac{2}{3}\varepsilon^{-1}\left(\frac{1}{\gamma} + \frac{\gamma-1}{\gamma}\frac{1+\varepsilon}{\varepsilon}\right)\frac{1}{\lambda} Ra, \quad \mathrm{Pr}_r = \left(\frac{1}{\gamma} + \frac{\gamma-1}{\gamma}\frac{1+\varepsilon}{\varepsilon}\right)\frac{1}{\lambda}\mathrm{Pr}, \quad Rv_r = \frac{4}{9}\varepsilon^{-2}\left(\frac{1}{\gamma} + \frac{\gamma-1}{\gamma}\frac{1+\varepsilon}{\varepsilon}\right)\frac{1}{\lambda} Rv \tag{3}$$

The last relations include Rayleigh, Prandtl numbers Ra, Pr, vibrational Rayleigh number Rv and the ratio of specific heats γ which don't depend on the vicinity to the critical point and defined by characteristics far from this point (characteristics of the perfect gas)

$$Ra = \theta' g' l'^3 \rho'^2 \frac{c_{v0}' + B'}{T'_c \lambda_0' \eta_0'}, \quad \mathrm{Pr} = \frac{(c_{v0}' + B')\eta_0'}{\lambda_0'}, \quad Rv = \frac{1}{2}\left(\frac{A'\omega'\Theta'\rho'_c l'}{T'_c}\right)^2 \frac{c'_{v0} + B'}{\eta'_0 \lambda'_0}, \quad \gamma = 1 + \frac{B'}{c'_{v0}} \tag{4}$$

Proceedings of the First International Symposium on Microgravity Research & Applications in Physical Sciences & Biotechnology, Sorrento, Italy, 10-15 September 2000. P. 229-234.

The subscript "0" denotes values in perfect gas; $B' = R'/\mu'_g$ is the constant of perfect gas R' per molecular weight μ'_g. Near-critical features are associated with parameter $\varepsilon = (T' - T'_c)/T'_c$ - the temperature distance from the critical point and with the coefficient of thermal conductivity which depends on ε and described as $\lambda = 1 + \Lambda\varepsilon^{-\Psi}$. Consequently the only temperature parameter ε is responsible for the near-critical properties indicated in "real" undimensional criteria. In near-critical region where $\varepsilon \to 0$ these criteria strongly increase and asymptotically diverge: $Ra_r \sim \varepsilon^{\Psi-2} \to \infty$, $\mathrm{Pr}_r \sim \varepsilon^{\Psi-1} \to \infty$, $Rv_r \sim \varepsilon^{\Psi-3} \to \infty$ ($\Psi < 1$).

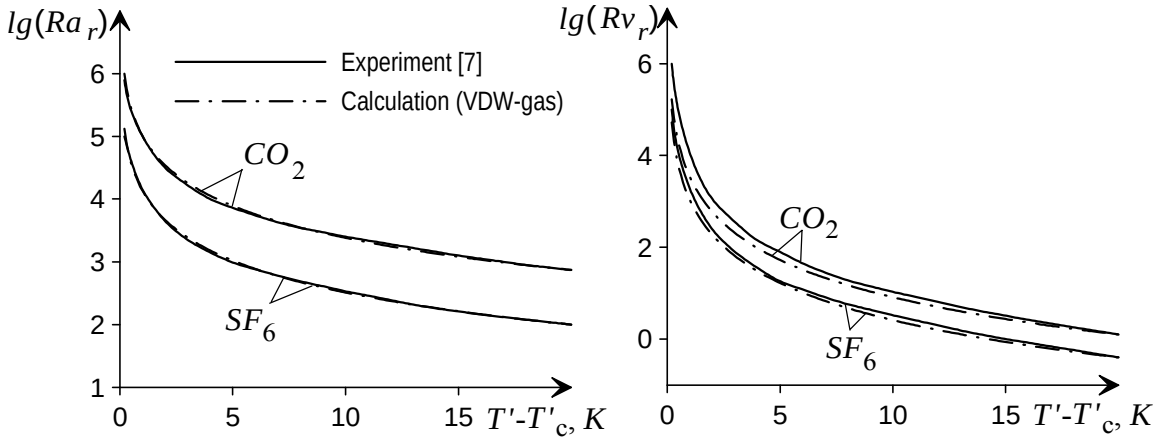

Fig.1. *Experimental and calculated "real" Rayleigh number Ra_r and vibrational Rayleigh number Rv_r as a functions of the temperature distance from the critical point $T' - T'_c$*

Fig. 1 represents the "real" Rayleigh number Ra_r and vibrational Rayleigh number Rv_r calculated with help of relations (3). These criteria are compared with values Ra_r and Rv_r defined on the experimental (variable with temperature) characteristics of the real fluids (CO_2 and SF_6) [7]. The results show a good agreement between criteria calculated on the basis of Van der Waals equation of state and they experimental analogies and prove the validation of applied mathematical model. On the other hand, fig. 1 demonstrates the strong dependence of the near critical processes on gravity because real criteria may increase on some orders and become in microgravity conditions the same as on the Earth for perfect gases.

Governing equations of the non-perfect gas

Navier-Stokes equations and equation of energy for non-perfect gas with arbitrary two-parametrical equation of state are applied. The approximation to low-speed flows is used therefore total pressure p is decomposed into two parts: equilibrium thermodynamical pressure p_e and dynamical pressure p_1; $p = p_e + 1/\gamma M^2 p_1$ (M - Mach number). To close the set of equations the integral mass balance is involved.

$$\frac{\partial \rho}{\partial t} + \nabla(\rho\vec{U}) = 0$$

$$\rho\frac{\partial \vec{U}}{\partial t} + \rho(\vec{U}\nabla)\vec{U} = -\nabla p_1 + \frac{1}{\mathrm{Re}}\left[2\nabla(\mu\dot{D}) - \nabla\left(\left(\frac{2}{3}\mu - \varsigma\right)\nabla\vec{U}\right)\right] + \frac{Ra}{\mathrm{Pr}\,\Theta\,\mathrm{Re}^2}(\rho - \rho_e)\vec{g}$$

$$\rho\frac{\partial T}{\partial t} + \rho(\vec{U}\nabla)T = -(\gamma - 1)T\left(\frac{\partial p_e}{\partial T}\right)_\rho \nabla\vec{U} + \frac{\gamma}{\mathrm{Re}\,\mathrm{Pr}}\nabla(\lambda\nabla T) \qquad (5)$$

$$p_e = p_e(\rho, T)$$

$$\int_V \rho\, dv = const$$

Stratification is described in linear approximation («e» - in equilibrium, «*» - on boundary):

$$\rho_e = \rho^* \left(1 + \left(\frac{\partial \rho^*}{\partial p^*} \right)_{T^*} \varepsilon_g \vec{g} (\vec{r} - \vec{r}^*) \right), \quad p_e = p^* + \rho^* \varepsilon_g \vec{g} (\vec{r} - \vec{r}^*) \tag{6}$$

Reynolds number $\mathrm{Re} = \rho_c' U' l' / \eta_0'$, temperature difference $\Theta = \Theta' / T'_c$ and parameter of hydrostatic compressibility $\varepsilon_g = g' l' / (B' T_c')$ arise in governing dimensionless equations (5)-(6) in addition to mentioned above parameters. To simulate heat and mass transfer in the frame of the model (5)-(6) equation of state should be defined. We use Van der Waals equation of state $p_e = \rho T / (1 - b\rho) - a\rho^2$ (a and b are constants) to describe near-critical fluid and equation of state $p_e = \rho T$ for perfect gas. This choice allows us to define derivatives $(\partial p_e / \partial T)_\rho$ in equation of energy (5) and $(\partial \rho^* / \partial p^*)_{T^*}$ in equation of density stratification (6).

Governing equations are solved numerically by novel program complex using finite difference implicit methods (SIMPLE-type method and others).

Thermal gravity-driven convection without vibrations

Thermal gravity-driven convection in square cavity with size $l' = 1\,cm$ subjected to side heating without vibrations is considered. Initially fluid is isothermal (with $T' - T'_c = 1\,K$) and at rest. Then temperature on the left side increases during 1 s to $0{,}1\,K$ and after this remains the same. Right boundary is isothermal, horizontal boundaries are adiabatic. Due to heat pulse input heat and mass transfer is developed in fluid. In the initial period this process is unsteady but in time it become steady. Near-critical unsteady problem in square cavity with side heating is realised previously for the case of one isothermal and other adiabatic boundaries [5]. In contrast with this situation when motion decays in time the maintaining of two opposite walls at different fixed temperatures leads to steady convection.

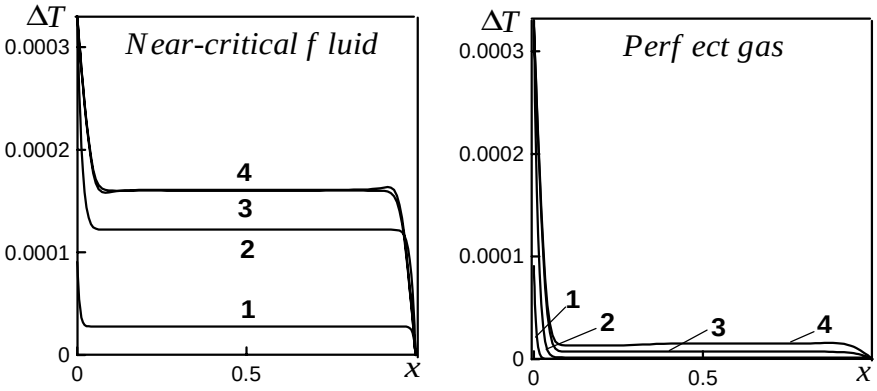

Fig.2. *Temperature differences ΔT in the central horizontal section at times t' =2,75 (1), 10 (2), 69 (3), 137 s (4)*

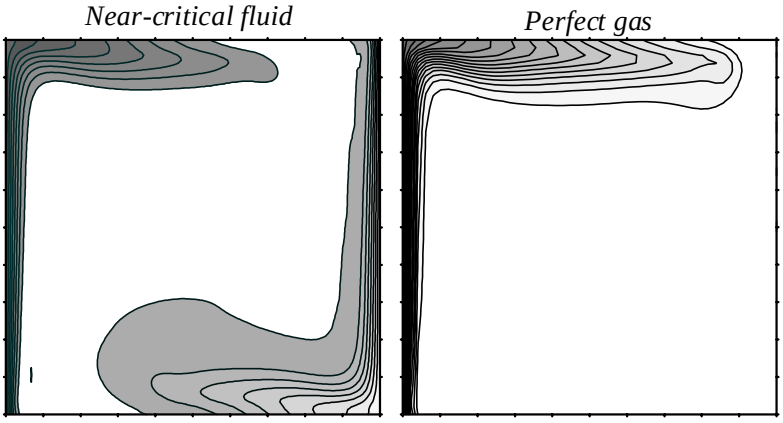

Fig.3. *Isotherms at time t' =69 s*

Numerical simulation was performed using undimentional criteria $\mathrm{Re} = 3{,}85 \cdot 10^4$, $\Theta = 3{,}3 \cdot 10^{-4}$, $\gamma = 1{,}4$, $\varepsilon_g = 2{,}86 \cdot 10^{-9}$, $\Lambda = 0{,}028$, $\psi = 0{,}74$ based on the scales $U' = 28{,}5\ cm/s$, $t' = 0{,}0351\ s$ and critical values. Two media were considered: near-critical fluid with $\varepsilon = 3{,}3 \cdot 10^{-3}$, $Ra = 10^3$, $\mathrm{Pr} = 1$ and perfect gas with essentially larger parameters which are equal to "real" parameters of the near-critical fluid calculated in (3) that is perfect gas with $Ra = 6{,}06 \cdot 10^6$, $\mathrm{Pr} = 30$.

During a short time near-critical fluid inside the cavity is heated rapidly due to piston effect. Because the vertical boundaries are supported at constant temperatures (after heating pulse) thermal boundary layers are formed – see fig. 2 (left picture). As a result upstream rises near the left warm surface and downstream moves near the cool right surface. This two-stream convective structure is shown in fig. 3 (left). Perfect gas is heated very slowly by means of diffusion and its temperature in the bulk doesn't increase sufficiently in compare with near-critical fluid (fig. 2). Gas inside the cavity remains cool for a long time, thermal boundary layer is formed only near heated side that leads to forming a single stream; fig. 3 (right) demonstrates this process.

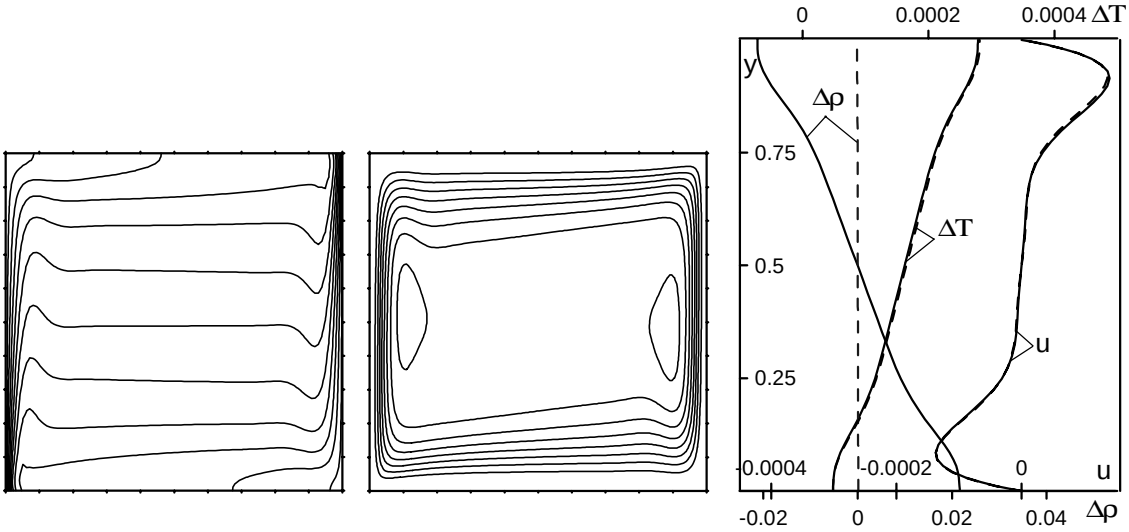

Fig.4. *Steady convection: isotherms (left), isolines of the stream function (centre) for near-critical fluid and perfect gas and distributions of different characteristics in the central vertical section (right) for near-critical fluid (solid lines) and for perfect gas (dashed lines)*

On the long time defined by characteristic time of heat diffusion convection in cavity become steady. Heat and dynamic fields of two media are similar (fig. 4, left, centre), but fields of density contrast with each other because of hypercompressibility in the near-critical fluid (fig. 4, right).

Thermal gravity-driven and vibrational convection

Thermal gravity-driven and vibrational convection of the near-critical fluid in microgravity is simulated. Left boundary of the cavity with initially isothermal fluid (its temperature is over the critical temperature on $0{,}5K$) is heated during 1 s to $0{,}1K$ then heating is stopped. Other boundaries are thermally isolated. As against problem above in this consideration cavity may oscillates along vertical axis that is given by the variable mass force in governing equations: $\vec{g} = (0,\ g_0 + A \cdot \cos \omega t)$. Oscillations have amplitude 1 mm and frequency 5 Hz and described by undimensional parameters $A = 0{,}1$, $\omega = 1{,}1$. Uniform part of mass force scaled by on-ground acceleration has value $g_0 = 3 \cdot 10^{-4}$ and produces Rayleigh number $Ra = 4{,}05 \cdot 10^2$. Thermal conductivity is specified by constants $\Lambda = 0{,}75$, $\psi = 0{,}5$.

To obtain characteristics of average motion the variables were calculated with help of full equations (5)-(6) then they were averaged over period of oscillations. Average large-scale convective motion is described by vibrational Rayleigh number $Rv = 2{,}2$ defined in (4). This value includes the physical parameters of perfect gas and as Ra doesn't characterise near-critical convection. Convection in this medium is characterised by the "real" criteria $Ra_r = 1{,}46 \cdot 10^6$ and $Rv_r = 3{,}24 \cdot 10^6$ calculated in (3) which are larger on the orders. They are the criteria which are responsible for the thermal gravity-driven and average vibrational convection in the near-critical fluid.

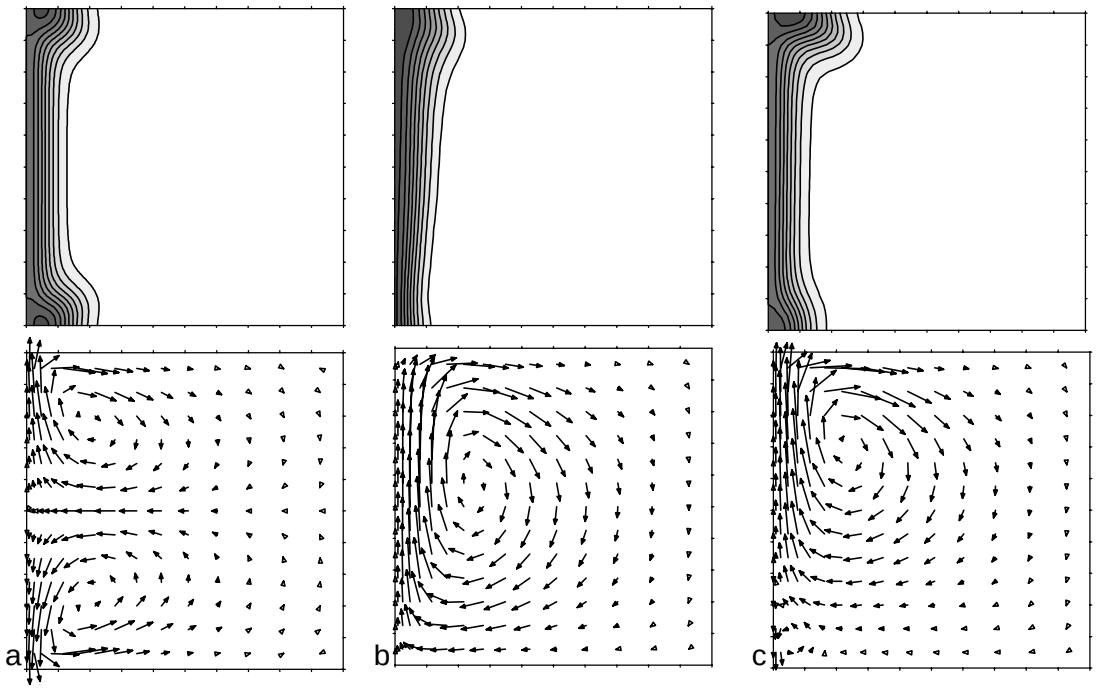

Fig.5. *Isotherms (upper) and velocity fields (bottom) at time* t' *=60 s under the influence of vibrational mass force (a), uniform mass force (b) and they superposition (c)*

Fig. 5 shows the results of simulation of near-critical convection in three cases: mass force is only oscillation ($g_0 = 0$), uniform ($A = 0$) and coupling. It may be seen that vibrational force induces symmetrical convective flow with two oppositely rotated vortices, action of uniform force leads to forming a single vortex from the upstream and more complicated asymmetrical structures are generated under superposition of two types of forces. Notice that as parameters of fluid approach to critical parameters, the vibrational convection becomes more intensive in comparison with thermal gravity-driven convection. It is clear because $Rv_r / Ra_r \sim \varepsilon^{-1} \to \infty$ when $\varepsilon \to 0$ (see equations (3)). This problem is discussed in more detail in [8].

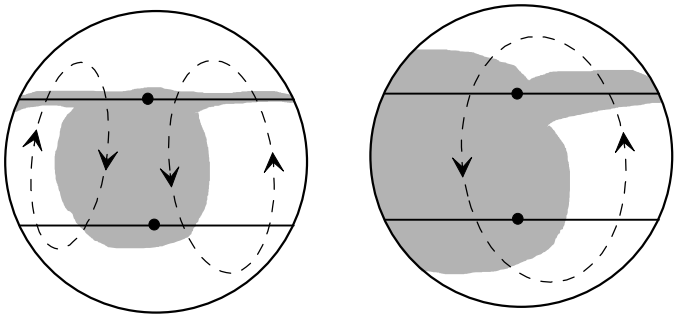

Fig.6. *Schemes of convection for the optical pictures obtained in a near-critical fluids at* $T'-T'_c = 0{,}121\ K$ *after heat input;* t' *=19 s (left), 65 s (right).*

Numerical results and analysis of the "real" criteria make it possible to qualitatively interpret the optical pictures obtained in a near-critical fluids onboard of the MIR station in experiments with Alice-1 instrument [7], [9]; schemes of convection are shown in fig. 6 [7]. Real microgravity in the MIR station has high-frequency component with amplitude $10^{-6} \div 10^{-3}\ g_e$ (g_e is the gravitational acceleration on the Earth) and frequency $0{,}1 \div 14$ Hz [7]. These values agree with vibrational Rayleigh number not over $Rv = 2 \cdot 10^{-3}$ which is too small. But fluid has parameters very close to critical (temperature distance $T'-T'_c = 0{,}121 K$ and $\varepsilon \approx 3 \cdot 10^{-4}$) because it characterised by "real" number with large value up to $Rv_r = 6 \cdot 10^5$. Thanks to this large value high-frequency component of real microgravity may induce the vibrational type of convection in near-critical fluids. Quasi-steady component of microgravity may disturb flow forming more complete asymmetrical structures.

Conclusions

Heat and mass transfer in near-critical fluid was considered. Numerical simulation of the near-critical thermohydrodynamics was performed on the basis of Navier-Stokes equations for the real gas with arbitrary two-parametrical equation of state in approximation to low-speed flows. Near-critical fluid was described with help of van der Waals equation of state. To interpret heat transport and convective motion in such media and to compare they with perfect gas the "real" undimensional criteria based on the near-critical properties were introduced. It was shown that "real" calculated criteria are in a good agreement with they experimental analogies that proves the validation of this mathematical model.

Thermal gravity-driven convection in a square cavity with side heating in near-critical fluid and in perfect gas was simulated. Undimensional criteria in governing equations for two media were different but criteria of perfect gas were found as equal to "real" criteria of near-critical fluid. Results demonstrated that initial unsteady heat and mass transfer in two cases has qualitative distinctions and essentially defined by the piston effect in near-critical fluid. In steady convection heat and dynamic field are similar, but fields of density contrast with each other owing to hypercompressibility near critical point.

Thermal vibrational convection, gravity-driven convection and superposition of these two types of motion were simulated. Comparison with experimental optical pictures from MIR station explained possibility of vibrational average motion in near-critical fluids. It is possible because as obtained "real" vibrational Rayleigh number may be very large even for microaccelerations.

This work was supported by the Russian Foundation for Basic Research, Grant № 00-01-00401.

Literature

1. H. E. Stanley. *Introduction to Phase Transition and Critical Phenomena.* Oxford University Press, London, 1971.
2. A. Onuki, H. Hao and R.A. Ferrell. Fast Adiabatic Equilibration in a Single-Component Fluid near the Liquid-Vapor Critical Point. *Phys. Rev.* A **41** (1990), 2256-2259.
3. B. Zappoli, A. Durand-Daubin. Heat and Mass Transport in a Near Supercritical Fluid. *Phys. Fluid.* **6**, № 5 (1994), 1929-1936.
4. T. Maekava, K. Ishii and S. Masuda. Temperature Propagation and Cluster Structures in a Near-Critical Fluid. *Joint 1st Pan-Pacific Basin Workshop and 4th Japan-China Workshop on Microfravity Sciences Proceedings. J. Jpn. Soc. Microgravity Appl*. **15-II** (1998), 130-135
5. B. Zappoli, S. Amirodine, P. Carles, J. Ouazzani. Thermoacoustic and Buoyancy-Driven Transport in a Square Side-Heated Cavity Filled with a Near-Critical Fluid. *J. Fluid Mech.* **316** (1996), 53-72.
6. E.B. Soboleva. On the Influence of Equation of State on the Near-Critical Heat and Mass Transfer Simulation. *High Temperature Thermophysics.* **38**, № 5 (2000), 1-7 (russian).
7. Zyuzgin A.B., Ivanov A.I., Polezhaev V.I., Putin G.F. On the Near-Critical Convection in Real Microgravity Onboard of the MIR Station. *Vibrational effects in hydrodynamics.* Perm, PGU, 2000 (russian).
8. V.I. Polezhaev, E.B. Soboleva. Thermal gravity-driven and vibrational convection in near-critical fluid in enclose with side heating. *Izvestia RAN, MZnG.* № 2 (2000), 70-80 (russian; transl. as *Fluid Dynamics*).
9. S.V. Avdeev, A.I. Ivanov, A.V. Kalmykov, A.A. Gorbunov, S.A. Nikitin, V.I. Polezhaev, G.F. Putin, A.V. Zuzgin, V.V. Sazonov, D. Beysens, Y. Garrabos, T. Frohlich, B. Zappoli. *Experiments in the Far and Near Critical Fluid Aboard MIR Station with the Use of the "ALICE-1" Instrument.* Proceedings of the Joint X-th European and VI-th Russian Symposium on Physical Sciences in Microgravity. St.-Petersburg, Russsia, **I** (1997), 333-340.